

Title:

ELECTRON PROTON TWO-STREAM INSTABILITY AT THE PSR

Author(s):

R. J. Macek, A. Browman, D Fitzgerald, R. McCrady,
F. Merrill, M. Plum, T. Spickermann, T. S. Wang,
J. Griffin, K.Y. Ng, D. Wildman, K. Harkay, R. Kustom
and R. Rosenberg

Submitted to:

<http://lib-www.lanl.gov/la-pubs/00796417.pdf>

ELECTRON PROTON TWO-STREAM INSTABILITY AT THE PSR*

R. J. Macek[†], A. Browman, D Fitzgerald, R. McCrady, F. Merrill, M. Plum, T. Spickermann and
T. S. Wang, LANL, Los Alamos, NM 87545, USA
J. Griffin, K.Y. Ng, D. Wildman, FNAL, Batavia, IL 60510, USA
K. Harkay, R. Kustom, R. Rosenberg, ANL, Argonne, IL 60439, USA

Abstract

A strong, fast, transverse instability has long been observed at the Los Alamos Proton Storage Ring (PSR) where it is a limiting factor on peak intensity. Most of the available evidence, based on measurements of the unstable proton beam motion, is consistent with an electron-proton two-stream instability. The need for higher beam intensity at PSR [1] and for future high-intensity, proton drivers has motivated a multi-lab collaboration (LANL, ANL, FNAL, LBNL, BNL, ORNL, and PPPL) to coordinate research on the causes, dynamics and cures for this instability. Important characteristics of the electron cloud were recently measured with retarding field electron analyzers and various collection electrodes. Suppression of the electron cloud formation by TiN coatings has confirmed the importance of secondary emission processes in its generation. New tests of potential controls included dual harmonic rf, damping by higher order multipoles, damping by X,Y coupling and the use of inductive inserts to compensate longitudinal space charge forces. With these controls and higher rf voltage the PSR has accumulated stable beam intensity up to 9.7 $\mu\text{C}/\text{pulse}$ (6×10^{13} protons), which is a 60% increase over the previous maximum.

1 INTRODUCTION

Since 1991, the working model of the e-p instability at PSR has been Neuffer's picture [2], which combined the analytical features of a coasting-beam, centroid model first developed by Zotter [3], and trapping of electrons by a small amount of beam in the gap. The model is qualitatively consistent with the available evidence, which primarily came from observations of the unstable beam motion. Some of the most compelling evidence is the frequency spectra of the unstable beam motion at threshold; an example of which is shown in Fig. 1. The mean frequency occurs at the calculated electron "bounce" frequency (in the field of the proton beam) and varies with the square root of intensity as predicted.

One of the longstanding unknowns for the e-p instability at PSR has been the origin and characteristics of the electron cloud. Past efforts to identify the dominant source(s) of the electrons and the degree of neutralization of the beam, which are not predicted in the Neuffer

model, have produced puzzling and inconclusive results. Significant changes in several well-known sources of electrons have had little effect on the instability. For example, increasing the vacuum pressure by factors of 10 to 100 produced insignificant changes in the instability threshold intensity. Likewise, increases in the beam losses by factors of 2-3 had no effect. Suppression of electrons in the injection section by various clearing fields also had only a modest effect on the instability.

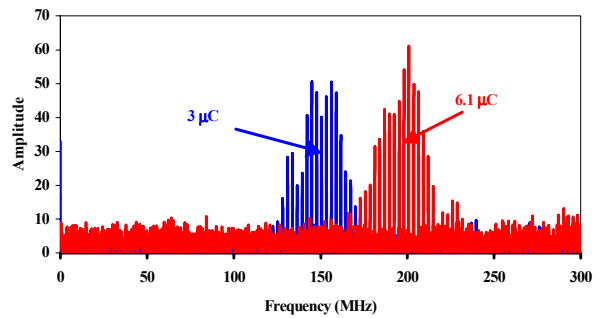


Figure 1. Frequency spectra at threshold for two intensities, 6.1 and 3 $\mu\text{C}/\text{pulse}$.

2 ELECTRON CLOUD STUDIES

Some evidence for an avalanche of electrons associated with unstable beams had been observed with biased collection plates. However, the charged plates perturb the electron and beam environment and may significantly change the electron cloud characteristics. Fortunately, improved detection and characterization of the electrons striking the wall was made possible by use of several retarding field analyzers (RFA) developed at ANL [4]. These were designed to introduce minimal perturbations to the beam and electron cloud. When augmented by high-speed electronics developed at LANL, these devices enable one to measure the flux density, time structure and energy spectra of electrons striking the wall [5].

2.1 RFA Signals

Over time, a number of these devices were placed at various locations in the ring including:

- a straight section in a low beam-loss region,
- a straight section in a high loss region,
- downstream of the injection stripping foil, and
- in a straight section which contained short ceramic breaks in the beam pipe.

These were augmented with small collection plates for use in dipole and quadrupole magnets.

*Work conducted by the Los Alamos National Laboratory, which is operated by the University of California for the United States Department of Energy under contract W-7405-ENG-36.

[†]macek@lanl.gov

A representative set of signals from an RFA detector observing a stable beam ($\sim 8 \mu\text{C}/\text{pulse}$) is shown in Fig. 2. Signals for several values of the repeller voltage from -300 V to $+25 \text{ V}$ are plotted. These detectors collect electrons with energies higher than the value set by the negative repeller voltage, thus providing data on the cumulative energy spectrum, which in this case extends out just beyond 300 eV . From these signals, it is apparent that most of the electrons strike the wall in a relatively short pulse at the end of the beam pulse. In general, the higher energy electrons are in a shorter pulse. The long tail on the signal for the $+25 \text{ V}$ repeller setting undoubtedly includes secondary and tertiary electrons produced by the impact of higher energy electrons.

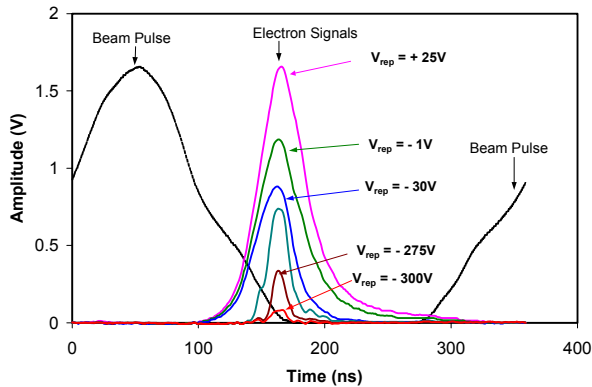


Figure 2. Electron signals during a single revolution plotted in time relation to the beam pulse.

The observed electron flux density is high compared with that expected from residual gas ionization. The peak of the signal for a repeller voltage of $+25 \text{ V}$ corresponds to $\sim 400 \mu\text{A}/\text{cm}^2$ striking the wall at this detector. This is five orders of magnitude higher than the $\sim 2 \text{ nA}/\text{cm}^2$ expected from residual gas ionization, assuming that the electrons generated in the passage of one beam pulse emerge in a pulse $\sim 40 \text{ ns}$ wide at the end of each beam pulse.

2.2 Factors Influencing Electron Flux

Numerous studies were made of the dependence of electron signals (for stable beams) on a variety of beam and environmental factors including location, beam intensity, pulse shape, local beam losses and vacuum pressure [5], [6]. It was found that the electron flux increases strongly with beam intensity as well as with local beam losses and vacuum pressure. In addition, the flux density varies markedly with beam shape. The very strong dependence on beam intensity is illustrated in Fig. 3 where the filtered electron signal (averaged over a few turns) is plotted as a function of the circulating beam intensity measured during accumulation in the ring. A power law fit to this data showed the electron flux density striking the wall varied as the 5.6 power of the beam intensity. For stable beams of intensities greater than $\sim 5 \mu\text{C}/\text{pulse}$, large electron signals were observed wherever diagnostics were placed including inside dipole

and quadrupole magnets. Essential electron cloud characteristics such as the dependence on beam intensity are not the same at all locations in the ring for reasons not completely understood at this time. The differences could imply sensitivity to local environmental factors (e.g. surface chemistry) or another production mechanism.

Factors of 2 to 10 more electrons are observed with unstable beams while other characteristics are similar to those for stable beams; in particular, most electrons still emerge at the end of the pulse. Interestingly, the excess of electrons (over that for a stable beam of the same intensity) is observed during the unstable beam motion but not before the motion becomes unstable.

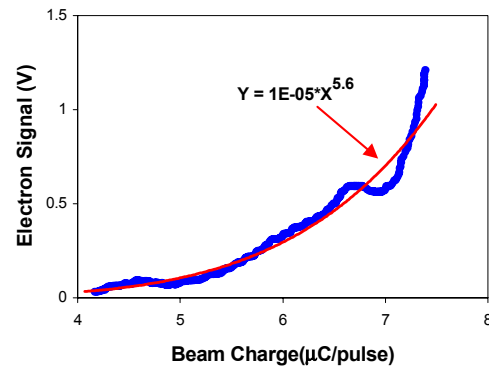


Figure 3. Electron yield as a function of beam intensity.

It has been suspected for some time that a type of beam induced multipactor or secondary emission avalanche at the vacuum walls plays a role in generating the electron cloud at PSR. If so, suppression of the secondary emission yield by TiN coatings could reduce the electron cloud generation. In an important test at PSR, TiN coating of a 2.7 m straight section gave a factor of 100 suppression of the observed electron signal and strongly suggests the crucial role of secondary emission in electron generation.

Increases in vacuum pressure have been taken as evidence for beam induced multipactor at certain other machines. In an experiment at PSR using high intensity pulses ($\sim 8.2 \mu\text{C}/\text{pulse}$) at low repetition rate ($\sim 0.2 \text{ Hz}$), the pressure changed from $4 \times 10^{-9} \text{ Torr}$ before the beam pulse to a peak of $3.5 \times 10^{-8} \text{ Torr}$. The pressure excursion had a rise time $\sim 8 \text{ ms}$ and a decay time of $\sim 0.5 \text{ s}$. At $6.7 \mu\text{C}/\text{pulse}$, the pressure pulse was down a factor of ~ 5 , which is roughly consistent with the change in electron flux striking the wall (assuming that the electrons cause a release of adsorbed gas from the walls roughly proportional to the electron flux striking the walls).

A conditioning effect on the threshold for the e-p instability has been observed on several occasions since 1997 [6]. In the past year, a more systematic effort was made to quantify the effect beginning with the startup after a several month shutdown during which parts of the ring were up to air. These data show an improvement by a factor of 2-3 in the threshold intensity over time suggesting that the electron flux striking the wall scrubs the surface and lowers the secondary emission yield (SEY) over time. [7]

2.3 Mechanisms for Electron Generation

Two candidate mechanisms for explaining the observed production of the PSR electron cloud have been considered. In the first, electrons captured by the beam (e.g. from residual gas ionization or electrons that survive the gap) oscillate in the potential well of the proton beam. They emerge at the end of the pulse with energies that depend on initial conditions and beam intensity but can range up to ~ 200 eV for $8 \mu\text{C}/\text{pulse}$ beams. When these strike the wall, secondaries are produced with yields that can be greater than unity. The secondaries can travel to the opposite wall and reflect or make tertiary electrons. These interactions with the wall will degrade the electron energies to a few eV in which case it can take many nanoseconds for them to die out. If a large enough fraction survives the gap, there will be an accumulation or buildup until the production and loss rates are in equilibrium.

A second candidate mechanism is based on what is aptly described as "trailing edge multipactor". Electrons born at the wall near or after the peak of the pulse will be accelerated towards the center of the beam and be decelerated after passing through the beam center. On the trailing edge of the beam pulse, such electrons will reach the opposite wall with some energy gain. If the energy gain is high enough, then the secondary emission yield can exceed unity and result in amplification on each successive traversal of the beam pipe. For an $8 \mu\text{C}/\text{pulse}$ triangular beam, a calculation indicates gains of ~ 1000 are possible for an electron born at the wall and at the peak of the beam pulse [8].

2.4 Single-Pass Experiment

One way to separate the contributions of the two mechanisms is to measure electrons from the passage of a single beam pulse in the PSR extraction line. No accumulation from previous pulses is possible. Results for such an experiment are shown in Fig. 4.

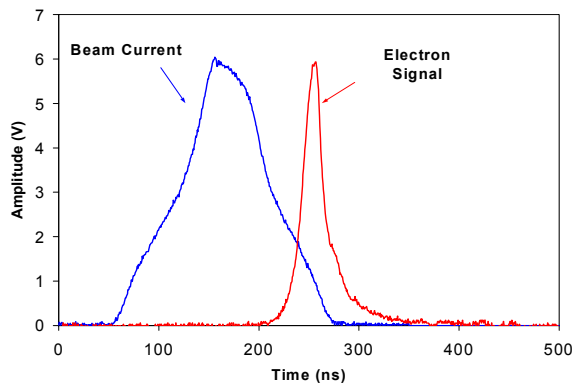


Figure 4. Electron signal compared to a $6.8 \mu\text{C}$ beam pulse in a single pass experiment ($V_{\text{rep}} = +25$ V).

There is a strong electron signal with a pulse shape and time relationship to the beam pulse that is nearly identical to those observed in the ring. Varying the repeller voltage

produces smaller and narrower electron signals, which disappear around -300 volts or so on the repeller, which is also similar to that observed in the ring. In addition, the electron signal is a very strong function of beam intensity. A power law fit to the data on intensity dependence required an exponent of 7, which is also similar to that observed in a straight section in the ring. These results strongly support the hypothesis that trailing edge multipactor is the dominant source of electrons striking the vacuum chamber wall in straight sections.

2.5 Estimates of Electron Density in the Beam

A large amount of data has been collected on the electron cloud in PSR of which only a small sample has been presented here [5],[6]. Interpretation in terms of the electron density in the beam is critical for comparison with e-p theory but is not straightforward or unique. The RFA only measures the electrons striking the wall, not the electron density in the beam. To infer electron cloud properties in the beam, a model is needed that can be fit to these data for the unknown parameters.

Electrons from trailing edge multipactor may cause large signals at the wall but contribute with a low weight to the electron density in the beam since they pass only once through the beam with a short dwell time (~ 5 ns) compared to captured electrons (~ 250 ns). Cold electrons, captured from the gap, contribute with a high weight since they oscillate against the protons throughout the passage of the beam pulses and are likely to be more important to the instability dynamics. Hence, an important unknown is the number of electrons that survive the gap to be captured by the next pulse. The electron signals in Fig. 2 show that a few percent of the low-energy electron signal is present at the beginning of the next beam pulse. Undoubtedly, more cold electrons are still in the pipe at smaller radii as indicated in a simulation developed by M. Furman and M. Pivi at LBNL. [9]

A numerical example of a neutralization estimate using the data shown in Fig. 2 for $V_{\text{rep}} = +25$ V is informative. Integration over time yields an electron flux of $23 \text{ pC}/\text{cm}^2/\text{turn}$. If all of the electrons are from captured electrons and their secondaries, then the estimated electron line density in the pipe is $\sim 340 \text{ pC}/\text{cm}/\text{turn}$ implying an average neutralization of 27%. If all observed electrons are from trailing edge multipactor, then the estimated average electron line density is $\sim 7 \text{ pC}/\text{cm}/\text{turn}$ implying $\sim 0.6\%$ neutralization. The true value probably lies somewhere in between, perhaps 2-3%.

From the discussion above, it is apparent that an experimental measure of the electrons surviving the gap would be a useful lower bound on the average neutralization. The design layout of a device [10] under construction at PSR is shown in Fig. 5. The concept is to use a pulsed electrode opposite a large area RFA to sweep electrons from the pipe into the RFA detector where they are collected. The timing of the short (~ 20 ns) pulse on the electrode selects the sampling time in the gap. The larger aperture of the entrance to the RFA will give a sensitivity that is ~ 8 time higher than the other RFA's in

use at PSR. The device will be installed and exploited in PSR in the summer of 2001.

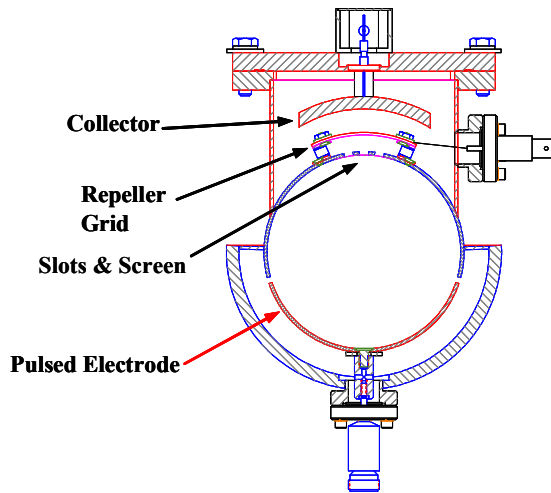


Figure 5. Cross-section of the electron sweeping detector.

4 TESTS OF POSSIBLE CURES

The twin themes of Landau damping and electron trapping by beam in the gap, which motivated many previous experiments and were used to interpret much of the available data, also inspired several potential cures that were studied, tested and found effective at PSR. These included:

- Higher rf buncher voltage made possible by improvements to the rf buncher system,
- Landau damping with sextupole and octupole fields
- Coupled Landau damping using a skew quadrupole,
- The use of inductive inserts to passively compensate longitudinal space charge forces.

A third theme, control by suppression of electron production, has proven very difficult to implement everywhere in the ring and has produced, at best, only modest improvement in the instability threshold intensity.

Following a proposal by J. Griffin, and in collaboration with Fermilab, inductive inserts constructed from ferrite rings [11] were tried and found to be effective in raising the instability threshold. The idea was to passively compensate longitudinal space charge in an effort to keep beam from leaking into the gap. Inductive inserts are equivalent to adding more rf voltage (with appropriate harmonics) which also increases the momentum spread and therefore should provide additional Landau damping.

A quite useful measure of the effect of various controls is the instability threshold intensity curve, where the stored beam intensity at the threshold for instability is plotted as a function of rf buncher voltage as shown in Fig. 6. The lowest curve was obtained for the ring with no inductors installed and with the sextupoles set to zero current. After installation of sufficient inductance to fully compensate longitudinal space charge, the instability threshold curve was raised significantly (middle curve). Further improvement was obtained when the sextupoles were turned on and optimized (highest curve).

Transverse (X,Y) coupling via a skew quadrupole was found to be surprisingly effective as shown in Fig. 7. According to Metral's theory of coupled Landau damping [12], transverse coupling shares the stabilizing tune spreads and growth rates in both planes thereby providing extra damping.

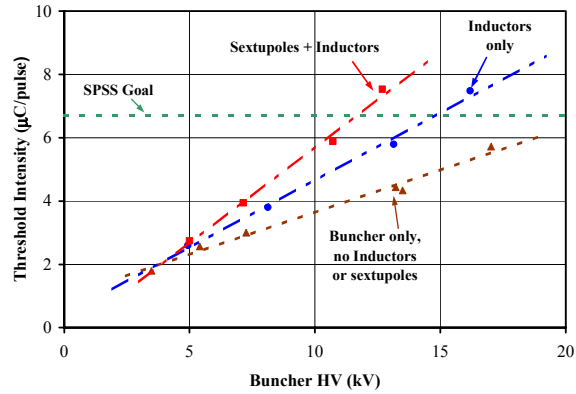


Figure 6. Effect of inductive inserts and sextupoles on the instability threshold-intensity curves.

The effect of sextupoles and octupoles is very similar to the effect of the skew quadrupole. All decrease the threshold buncher voltage and increase beam losses. The strategy for PSR is to use each of these devices at low excitation where the losses haven't increased appreciably but where the effect on the instability is sizeable. It is hoped that the suppression of the instability from all these devices is additive. To date, the pair-wise effect of sextupoles and inductors or a skew quadrupole and inductors has been demonstrated to combine favorably.

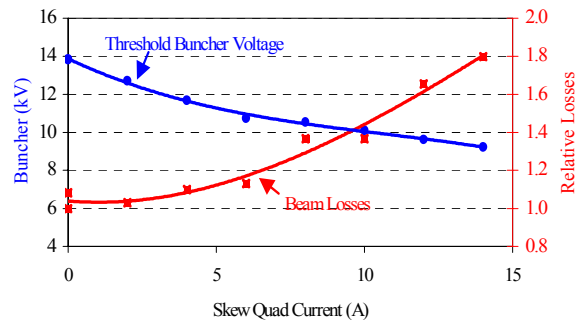


Figure 7. Instability threshold voltage and relative beam losses as a function of skew quad current for fixed beam intensity (stored charge of 5 $\mu\text{C/pulse}$).

The program of tests culminated in demonstration of a record, stable beam store of **9.7 $\mu\text{C/pulse}$** , which is 45% higher than needed to meet the SPSS enhancement project peak intensity specification of 6.7 $\mu\text{C/pulse}$ [1]. The demonstration at low repetition rate was made using the combined effect of the maximum available rf voltage (18 kV), heated inductors ($\sim 190^\circ\text{C}$), and a skew quadrupole. To accumulate this intensity with the existing H⁻ ion-source, the beam gate was stretched out to 1225 μs (50-60 % higher than normal), which can be done at low repetition rates.

The record accumulation produced a peak circulating current of 82 A that was still stable after an additional 400 μ s store at the end of accumulation. While the demonstration showed adequate control of the instability at high peak intensities, the beam losses were too high for routine operation. In addition, considerable emittance growth, presumably from space charge effects, was observed at the higher peak intensities

5 CONCLUSIONS

The wealth of data recently collected on the electron cloud in PSR has lead to important new insights regarding its origin. To date, however, there is only a partial explanation of the observations. More importantly, there is no unique interpretation in terms of electron density in the beam. The latest evidence does suggest that the "trailing edge multipactor" mechanism is the source of most of the observed electron signal striking the vacuum chamber walls in straight sections (about 40% of the circumference) but it is not certain that these electrons are the dominant contribution to the average electron density in the beam or to the electrons that drive the instability. Electrons observed in magnets and those near the stripper foil have significantly different characteristics and are not as well studied. The differences could be very important to the instability. Detailed simulations of the electron cloud generation [9] along with data from the new electron-sweeping detector, which is designed to measure the electrons surviving the gap, could help resolve these issues.

TiN coatings have greatly reduced the observed electron signal in the one straight section where they were tested. As such, they offer the prospect of a cure with no increase in losses. The experience to date (large electron signals at all locations) suggests that it may be necessary to coat the entire ring in order to cure the instability. This would be a major undertaking and is not likely in the near future.

Progress on understanding the e-p instability would be greatly aided by major improvements to the rigid, coasting beam, centroid model that has been the guiding picture for the work to date. Recent theoretical work is showing considerable promise. Modifications for a bunched beam have been explored analytically [13] and there is good progress on a fully kinetic model based on solutions of the Vlasov-Maxwell equations. [14]

Recent progress on control of the instability at PSR seems largely due to Landau damping but reduced beam in the gap may play a role that has proven difficult to isolate. Increased rf voltage, X,Y coupling, multipoles and inductive inserts have significantly raised the instability threshold. These are more than sufficient to meet the peak intensity specification for the PSR upgrade project but at the cost of increased losses. Thus, the main remaining challenge for the PSR upgrade and beyond is to find ways to control the instability while reducing the uncontrolled beam losses at higher intensities.

6 ACKNOWLEDGEMENTS

We gratefully acknowledge the contributions from D. Olsen, S. Danilov and J. Jones in providing vacuum chambers for the TiN tests and D. Wright for TiN coating of the test chambers. The corresponding author also acknowledges many helpful discussions with other members of the PSR e-p collaboration including M. Furman, M. Pivi, G. Lambertson, M. Blaskiewicz, R. Davidson, H. Qin, and P. Channell.

7 REFERENCES

- [1] The LANL SPSS Project, LAUR-98-4172, (1998).
- [2] D. Neuffer et al, "Observations of a Fast Transverse Instability in the PSR", NIM A 321 (1992), p. 1-12.
- [3] B. Zotter, "Landau-damping of coupled electron-proton oscillations", CERN-ISR-TH/71-58.
- [4] R. Rosenberg and K. Harkay, "A rudimentary electron energy analyzer for accelerator diagnostics", NIM A 453 (2000) p507-513.
- [5] A. Browman, "Electrons at PSR", Presentation at the 8th ICFA Mini Workshop on Two-Stream Instabilities in Particle Accelerators and Storage Rings Santa Fe, NM Feb 16-18, 2000. Proceedings are on the website: <http://www.aps.anl.gov/conferences/icfa/two-stream.html>.
- [6] R. Macek et al, "New Developments on the e-p Instability at the Proton Storage Ring (PSR)", ICANS-XV, Nov 6-9, 2000, p 229, Proc. ICANS-XV.
- [7] N. Hilleret, "Study of Surface Characteristic Determining Electron Cloud Growth"; also R. E. Kirby, "Secondary Electron Emission From Accelerator Materials", 8th ICFA Mini Workshop, Santa Fe, NM.
- [8] R. Macek, "Sources of electrons for stable beams in PSR", PSR Technical Note, PSR-00-10; also V. Danilov et al, "Multipacting on the Trailing Edge of Proton Beam Bunches in PSR and SNS", Workshop on Instabilities of High Intensity Hadron Beams in Rings, Upton, New York, June/July 1999, AIP Conf. Proceedings 496, p. 315.
- [9] M. Furman, et al, "Simulation Results for the Electron-Cloud at the PSR", Proc. PAC2001.
- [10] A. Browman, private communication and T.S. Wang, et al, "The Static Electric Field of a Curved Electrode in a Beam Pipe", PSR Technical Note 01-003 (2001).
- [11] M. A. Plum, et al, "Experimental study of passive compensation of space charge at the Los Alamos National Laboratory Proton Storage Ring", Phys. Rev. ST Accel. Beams 2, 064210 (June 1999). Also, K.Y. Ng, et al, "Recent Experience with Inductive Inserts at PSR", Proc. PAC2001.
- [12] E. Metral, "Theory of Coupled Landau Damping", Particle Accelerators, vol. 62(3-4), p. 259, January 1999.
- [13] T. S. Wang, et al, "Transverse Electron-Proton Two-Stream Instability in a Bunched Beam", Proc. PAC2001.
- [14] H. Qin, et al, "3D Simulation Studies of the Two-Stream Instability in Intense Particle Beams Based on the Vlasov-Maxwell Equations", Proc. PAC2001.